Scientific Research Publishing

Advances in Chemical Engineering and Science, 2016, 6, 379-398
http://www.scirp.org/journal/aces
ISSN Online: 2160-0406
ISSN Print: 2160-0392

Spectroscopic Elucidation of the Links between Char Morphology and Chemical Structure of Coals of Different Ranks

Andrew O. Odeh

Coal Research Group, Unit of Energy Systems, School of Chemical and Minerals Engineering, North-West University, Potchefstroom Campus, Potchefstroom, South Africa
Email: odehandy@yahoo.com

How to cite this paper: Odeh, A.O. (2016) Spectroscopic Elucidation of the Links between Char Morphology and Chemical Structure of Coals of Different Ranks. *Advances in Chemical Engineering and Science*, **6**, 379-398.
http://dx.doi.org/10.4236/aces.2016.64038

Received: August 30, 2016
Accepted: September 27, 2016
Published: September 30, 2016

Abstract

In this investigation, SAXS and XRD were used to investigate both the physical and chemical changes in six coals of different ranks subjected to heat treatment. The specific surface area which gives an indication of the reactivity of the coal (measures surface area available for reaction) was determined to be in the range of 70.04 - 260.40 m^2/cm^3 particle volume for lignite from 450˚C - 700˚C. The specific surface area was determined to be in the range of 51.58 - 239.00 m^2/cm^3 particle volume for sub-bituminous; 440.60 - 241.70 m^2/cm^3 particle volume for light volatile bituminous; 452.71 - 247.73 m^2/cm^3 particle volume for high volatile bituminous; 349.11 - 347.52 m^2/cm^3 particle volume for semi-anthracite and 333.60 - 125.34 m^2/cm^3 particle volume for anthracite respectively. On the other hand, the aromaticity was determined in the range of 0.66 - 0.76 for lignite; 0.67 to 0.80 for sub-bituminous; 0.91 - 0.97 for light volatile bituminous; 0.93 - 0.99 for high volatile bituminous; 0.96 - 1.00 for semi-anthracite and 0.96 to 0.99 for anthracite respectively. The porosity, pore size distribution associated with SAXS and the other crystallite parameters identified with XRD were also determined. Links between the physical and chemical parameters were established.

Keywords

Coal Char, Char Morphology, Chemical Structure, XRD, SAXS

1. Introduction

Pyrolysis is a critical initial step in the conversion of coal to other forms, whether by

combustion, gasification or liquefaction [1]. On subjecting coal particles to heat treatment, the coal particles undergo thermo-chemical decomposition with liberation of volatiles and the formation of a resultant solid residue, char. The reactivity of the char is dependent on both the physical and chemical changes that results from heat treatment of the coal particles. The role played by char in coal utilization processes has created a need for high quality; hence it is important to determine its chemical properties to ensure smooth operation [2] and high productivity of such processes as in fixed bed gasification [3]. The physical properties of coal which impact on coal conversion processes relate to those processes which results in charge of particle size [4] and surface morphology (density, pore size, pore size distribution) [5]. The chemical properties of coal which impact on the conversion processes are those which effect a change in the chemical constitution and these in turn may lead to changes in the physical properties such as the surface area [6]. It was generally found that increasing devolatilization temperature increases the structural orderliness of the resultant char carbon crystallite, which affects the lattice properties with increasing aromaticity [7]-[12]. Increase in aromaticity in coals indicates substantial chemical and spatial rearrangement [7] [9] [11]. It has generally been found that gasification and combustion reactivities decrease with increasing aromaticity [8]-[10]. Thus, thermal treatment leads to a more ordered and unreactive char matrix [12].

Increased volatile matter release creates fine pores [13], thus increasing the micropore porosity [14] and surface area [15]. All the changes indicate increased graphitization which can be expected to affect the intrinsic reactivity. The nature and extent of microstructural changes of a coal particle upon heat treatment depend on the coal composition [3]-[5] [16]. Low rank coals have the features of high concentration of oxygen-containing functional groups and high proportion of mesopores and macropores, and thus play a dual role of active and exchanging sites during coal utilization processes. At lower temperatures, the heterogeneous nature of coal is still evident in the char, having higher proportions of oxygen, hydrogen and disorganized carbon, while at higher coalification temperatures, atomic O/C and H/C ratios of char fall. This is due to progressive dehydrogenation and deoxygenation reactions as polycondensed aromatic structures are formed and polyaromatizaton (*i.e.* growth in the size of the aromatic sheets becomes dominant) [17]-[22].

Coal chars are comprised of non-uniform structures containing micro-, meso-, and marco-pores [17]. It is also reported that chars obtained under rapid heating conditions have rather porous structures [18]. It is reported that very low porosity may be in the chars obtained from coals with high inertinite and high mineral matter contents [19]. The porosity of chars is affected not only by intrinsic coal properties but also by pyrolysis conditions such as heating rate [20], temperature [21], and residence time [22]. Different behaviour of coals could originate from differences in their chemical structures: high rank coals consist of larger aromatic units with fewer ether and methylene bridges. The lower rank coals consist of smaller units with more numerous reactive ether and methylene linkages [23] [24]. Organic oxygen is an important component of the overall

structure and plays a key role in determining reactivity [2] [25]. Hence, a decrease in oxygen content in coal leads to energy content increasing automatically [26].

The pore structure of coal has long been the subject of intense interest and investigation and as such has been extensively researched [27]-[31]. This is in large part due to the importance of the pore structure to the passage of fluids in and out of coal, which naturally occur when coal is processed or burnt [27]. While the chemical structure of the coal determines the kinetics of the fluid-coal reaction at the surface, the porous structure dictates how much surface is available for reaction, and what role mass transfer will play in the overall rate of reaction [28] [29]. Conventional analytical techniques such as gas adsorption and mercury porosimetry has been employed in evaluating coal pore structures, however, these techniques comes with some limitations as data from these techniques often lead to incomplete and contradictory conclusions. Generally, adsorption works best when measuring surface areas of nonporous or macroporous substances with chemically homogenous surfaces. Mercury porosimetry equally works best with macroporosity [30] [31].

In this study, the internal and external structures of chars obtained at six pyrolysis temperature were characterized by small angle X-ray scattering (SAXS) and X-ray diffraction (XRD) respectively. The internal structure was characterized by determining the basic physical properties, as specific surface area, specific volume of pores, pore size distribution and porosity. The external structure was characterized by determining the basic chemical properties, as aromaticity, interlayer spacing and crystalline height. Both SAXS and XRD serve as attractive alternative characterization techniques because, above all, they are both nonintrusive (requiring little material and sample preparation). The SAXS readily penetrates the entire sample making it possible for pore size distribution (micropore, mesopore and macropore) to be evaluated in a single experimental run: the capability of measuring both closed and open porosity of carbonaceous materials such as coal [31] [32]. When X-rays penetrate materials, they are scattered off density contrasts within the material at a range of scattering angles [31]. The resulting scattering pattern, which is specific to the structure of the material can be analyzed to estimate surface areas and porosity features of the material [32]. Because SAXS scatters off density contrasts in coals, it not only scatters off density differences between the material and empty pores, but also scatters off density differences between their organic and inorganic components [31] [32]. To correct this anomaly, the coal could be demineralized to minimize the inorganic components.

While the XRD gives detail account of the crystallite features (aromaticity, interlayer spacing, and crystallite height) in an experimental run, SAXS accounts for the morphology of the carbonaceous material [33] [34]. Six coals of different ranks were used to investigate the coal to char transition and insights from the findings will be discussed. These coals covered a wide rank interval (lignite to anthracite) and have different maceral compositions. To achieve this, the selected coals were demineralized in order to study the effect of the organic part only and to establish links between the physical and chemical properties using spectroscopy technique.

2. Experimental

2.1. Sample Preparation

Six coals of varying rank were used: a lignite coal from Germany, coded as LIG; a sub-bituminous coal from Nigeria, coded as SUB; two bituminous coals from South Africa (one is low volatile bituminous, coded as BIT-LV and the other, high volatile bituminous coal, coded as BIT-HV); a semi-anthracite from South Africa, coded as SA; an anthracite from South Africa, coded as ANT. The coal samples were subjected to coal preparation and pulverized to coal particle size of −75 μm by employing a mechanical size reduction jaw crusher (Samuel Osborne (SA) LTD, model: 66YROLL) and a Fritsch P-14 rotary mill containing ceramic balls(Model number: 46 - 126). The required particle size of −75 μm was finally obtained from screening the particles from the rotary mill using a 75 μm screen All the samples were stored under argon in sealed bags.

The prepared coal samples were demineralised by sequential leaching with hydrofluoric acid (HF) and hydrochloric acid (HCl) The HF (48%) and HCl (32%) were obtained from Associated Chemical Enterprise (ACE), South Africa.

2.2. Apparatus and Procedure

The char production sequence from the parent coal samples are as follows: The weighed coal samples (40 g) were placed in a ceramic boat and put in a horizontal tube furnace at atmospheric conditions Initially, the samples were left for fifteen minutes and flushed with nitrogen (AFROX, ultra high pure grade) at atmospheric conditions, to remove oxygen from the oven. A flow rate of 1 liter/min of nitrogen was used. The furnace was then heated at 20˚C/min to the target temperature, and held isothermal for 60 minutes. The target temperature ranged from 450˚C to 700˚C, while keeping the samples under a nitrogen atmosphere.

The XRD experiments were done at XRD Analytical and Consulting, Pretoria, South Africa following the procedure and experimental method detailed in Everson and co-workers [35]. All the XRD experiments were repeated three times and the final results are averages of three independent results from which experimental errors were calculated at 95% confidence level. The surface areas of the various samples were determined using the carbon dioxide adsorption CO_2 DR method on a Micromeritics ASAP2020 surface area analyser [36]. Prior to CO_2 adsorption, the samples (about 0.20 gram) were degassed under vacuum (10.0 μmHg), at 380˚C for 48 hours for chars. The evacuated sample was analysed at 0˚C in an ice bath. The results were processed using the Accelerated Surface Area and Porosimetry System (ASAP) 2020 software linked to the Surface Area Analyzer. All the adsorption experiments were repeated three times and the final results are averages of three independent results from which experimental errors were calculated at 95% confidence level.

The char morphology were performed at Council of Scientific and Industrial Research (CSIR), South Africa, using the analytical technique of small angle X-ray scattering (SAXS), following the procedure and equipment at CSIR, Nano-Structured Ma-

terials Centre detailed in Calo and Hall [17]. All the SAXS experiments were repeated three times and the final results are averages of three independent results from which experimental errors were calculated at 95% confidence level.

3. Results and Discussion

Detailed characterization of the demineralized coal samples used in this study is presented in Table 1. As expected and as can be seen from the petrographic analysis in Table 1, the least value of 0.35 was obtained for the lignite coal (low rank) while the value of 2.94 was obtained for the anthracite coal (high rank) indicating that all the coal ranks were covered in this investigation. Detailed characterization of all chars consisting of results obtained from well-known standard analytical techniques such as CO_2 adsorption DR, SAXS and XRD are given in Tables 2-4, where chars are listed in the order of increasing rank. The chemical rank parameters as can be seen in Table 2 and Figure 1 followed the expected trend with increasing rank, that is, an increase in the crystallite height and aromaticity and a decrease in interlayer spacing. The crystallite height was determined to be in the range of 14 to 13 Å for the lignite char from 450˚C - 700˚C; 14 to 13 Å for sub-bituminous; 18 to 13 Å for light volatile bituminous; 16 to 13 Å for high volatile bituminous; 20 to 14 Å for semi-anthracite and 20 to 13 Å for anthracite.

The two low rank coals (lignite and sub-bituminous) seems to exhibit the same trend of slight decrease (a transformational change of 1 Å) of crystallite height with increasing pyrolysis temperature. The same story could be said of the other ranks; the two

Table 1. Properties of demineralized coal.

Coal	LIG	SUB	BIT-LV	BIT-HV	SA	ANT
Inherent moisture (air dried) wt%	1.7	1.9	1.3	2.7	2.3	2.5
Ash (air-dried) wt%	0.8	2.0	3.3	1.2	1.8	1.5
Volatile matter (air-dried) wt%	60.3	43.2	25.0	27.2	9.6	6.8
Fixed carbon (air-dried) wt%	37.3	53.0	70.4	68.9	86.3	89.2
Carbon (daf) wt%	69.2	75.1	80.9	83.4	89.0	85.6
Hydrogen (daf) wt%	6.2	5.2	4.2	4.6	3.3	2.4
Nitrogen (daf) wt%	0.6	1.8	2.3	2.0	1.8	2.0
Oxygen (daf) wt%	20.3	17.4	12.3	9.1	5.0	7.7
Sulphur (daf) wt%	2.7	0.1	0.3	1.0	0.7	2.1
Gross calorific value (MJ/kg)	28.9	29.3	30.0	32.0	33.3	32.7
Total reflectance (Ro)	0.35	0.77	1.27	1.23	2.45	2.94
H/C	1.08	0.83	0.62	0.66	0.45	0.34
O/C	0.22	0.17	0.11	0.08	0.04	0.07
f_a	0.40	0.58	0.74	0.72	0.84	0.98
Fuel ratio	0.6	1.2	2.8	2.5	9.0	13
DR surface area (m^2/g)	109	140	169	142	199	136

Table 2. Determined chemical properties of heat-treated coal (chars).

CHAR	LIGNITE (LIG)					
	450	500	550	600	650	700
Crystallite height (L_c) Å	14 ± 0.3	14 ± 0.3	14 ± 0.3	13 ± 0.3	13 ± 0.3	13 ± 0.3
Interlayer spacing (d_{002}) Å	3.67 ± 0.03	3.68 ± 0.02	3.70 ± 0.04	3.74 ± 0.01	3.76 ± 0.03	3.78 ± 0.03
Aromaticity (f_a)	0.66 ± 0.06	0.67 ± 0.07	0.68 ± 0.04	0.72 ± 0.05	0.74 ± 0.06	0.76 ± 0.04
	SUB-BITUMINOUS (SUB)					
Crystallite height (L_c) Å	14 ± 0.3	14 ± 0.3	14 ± 0.3	14 ± 0.3	13 ± 0.3	13 ± 0.3
Interlayer spacing (d_{002}) Å	3.66 ± 0.02	3.66 ± 0.01	3.66 ± 0.01	3.68 ± 0.02	3.71 ± 0.04	3.78 ± 0.03
Aromaticity (f_a)	0.67 ± 0.04	0.69 ± 0.05	0.70 ± 0.03	0.74 ± 0.06	0.78 ± 0.04	0.80 ± 0.06
	BITUMINOUS (BIT-LV)					
Crystallite height (L_c) Å	18 ± 0.3	17 ± 0.3	16 ± 0.3	15 ± 0.3	15 ± 0.3	13 ± 0.3
Interlayer spacing (d_{002}) Å	3.54 ± 0.01	3.56 ± 0.02	3.60 ± 0.04	3.61 ± 0.03	3.63 ± 0.03	3.64 ± 0.05
Aromaticity (f_a)	0.91 ± 0.08	0.94 ± 0.05	0.96 ± 0.04	0.97 ± 0.05	0.97 ± 0.07	0.99 ± 0.03
	BITUMINOUS (BIT-HV)					
Crystallite height (L_c) Å	16 ± 0.3	16 ± 0.3	16 ± 0.3	15 ± 0.3	15 ± 0.3	13 ± 0.3
Interlayer spacing (d_{002}) Å	3.55 ± 0.03	3.55 ± 0.02	3.56 ± 0.04	3.57 ± 0.05	3.58 ± 0.03	3.60 ± 0.06
Aromaticity (f_a)	0.93 ± 0.04	0.94 ± 0.07	0.97 ± 0.05	0.98 ± 0.05	0.98 ± 0.04	0.99 ± 0.06
	SEMI-ANTHRACITE (SA)					
Crystallite height (L_c) Å	20 ± 0.3	19 ± 0.3	18 ± 0.3	17 ± 0.3	15 ± 0.3	14 ± 0.3
Interlayer spacing (d_{002}) Å	3.47 ± 0.03	3.48 ± 0.04	3.51 ± 0.02	3.51 ± 0.02	3.51 ± 0.03	3.52 ± 0.04
Aromaticity (f_a)	0.96 ± 0.02	0.98 ± 0.05	0.99 ± 0.03	0.99 ± 0.04	0.99 ± 0.04	0.99 ± 0.03
	ANTHRACITE (ANT)					
Crystallite height (L_c) Å	20 ± 0.3	19 ± 0.3	18 ± 0.3	18 ± 0.3	17 ± 0.3	13 ± 0.3
Interlayer spacing (d_{002}) Å	3.47 ± 0.02	3.51 ± 0.03	3.51 ± 0.02	3.51 ± 0.03	3.52 ± 0.02	3.52 ± 0.04
Aromaticity (f_a)	0.96 ± 0.04	0.97 ± 0.02	0.98 ± 0.04	0.99 ± 0.02	0.99 ± 0.05	0.99 ± 0.03

medium rank coals exhibited same trend of gradual decrease (5 and 3 Å respectively) of crystallite height with increasing pyrolysis temperature while the high rank coals (SA and ANT) exhibited similar trend of gradual decrease (6 and 7 Å respectively) with increasing temperature. The interesting observation on the crystallite height is that, at the final pyrolysis temperature of 700˚C, there was a convergence to a value of 13 Å for all coal ranks. The decrease in crystallite height and the convergence to same value at higher pyrolysis temperature could be attributed to an increase in the number of aromatic layers as reported in Dangyu and co-workers [37] and an indication of no more effect of heat treatment on the coal [17]. Lu *et al.* [33] has reported that coal crystallites consist of 2 - 4 aromatic layers on average (basic structural units (BSU) in stacks of aromatic molecules). The interlayer spacing was determined to be in the range of 3.67 to 3.78 Å for LIG from 450˚C to 700˚C; 3.66 to 3.78 Å for SUB; 3.54 to 3.64 Å for BIT-LV; 3.55 to 3.60 Å for BIT-HV; 3.47 to 3.52 Å for SA and 3.47 to 3.52 Å for ANT.

The interlayer spacing demonstrated an increasing trend with increasing pyrolysis

Table 3. Determined physical properties of heat-treated coal (chars).

CHAR	LIGNITE (LIG)					
	450	500	550	600	650	700
Volume fraction (m^3/m^3)	0.366 ± 0.3	0.407 ± 0.2	0.509 ± 0.1	0.609 ± 0.2	0.423 ± 0.2	0.289 ± 0.1
Specific surface area (m^2/cm^3)	70.04 ± 5	71.86 ± 4	151.00 ± 5	162.20 ± 3	192.70 ± 6	260.40 ± 4
Radius of gyration (nm)	13.2 ± 0.2	14.0 ± 0.4	12.0 ± 0.2	13.2 ± 0.2	13.5 ± 0.3	15.5 ± 0.7
	SUB-BITUMINOUS (SUB)					
Volume fraction (m^3/m^3)	0.353 ± 0.1	0.358 ± 0.1	0.384 ± 0.3	0.424 ± 0.2	0.440 ± 0.2	0.423 ± 0.3
Specific surface area (m^2/cm^3)	51.58 ± 6	67.21 ± 4	77.69 ± 3	86.84 ± 2	192.00 ± 4	239.00 ± 3
Radius of gyration (nm)	14.7 ± 0.3	14.6 ± 0.3	14.1 ± 0.2	14.3 ± 0.4	14.6 ± 0.2	15.5 ± 0.2
	BITUMINOUS (BIT-LV)					
Volume fraction (m^3/m^3)	0.522 ± 0.2	0.619 ± 0.2	0.761 ± 0.2	0.679 ± 0.2	0.587 ± 0.1	0.585 ± 0.3
Specific surface area (m^2/cm^3)	440.60 ± 3	311.71 ± 7	219.50 ± 6	492.92 ± 3	334.10 ± 5	241.73 ± 4
Radius of gyration (nm)	13.7 ± 0.2	14.0 ± 0.2	14.1 ± 0.2	13.6 ± 0.2	13.5 ± 0.4	13.9 ± 0.2
	BITUMINOUS (BIT-HV)					
Volume fraction (m^3/m^3)	0.507 ± 0.3	0.607 ± 0.1	0.983 ± 0.1	0.849 ± 0.2	0.775 ± 0.1	0.676 ± 0.1
Specific surface area (m^2/cm^3)	452.70 ± 2	330.11 ± 6	62.49 ± 8	104.52 ± 3	109.61 ± 4	247.72 ± 2
Radius of gyration (nm)	13.7 ± 0.2	13.8 ± 0.4	14.0 ± 0.7	13.6 ± 0.2	13.9 ± 0.9	13.9 ± 0.3
	SEMI-ANTHRACITE (SA)					
Volume fraction (m^3/m^3)	0.583 ± 0.1	0.617 ± 0.2	0.750 ± 0.2	0.474 ± 0.1	0.812 ± 0.1	0.607 ± 0.2
Specific surface area (m^2/cm^3)	349.10 ± 2	145.21 ± 3	239.30 ± 3	127.72 ± 3	151.22 ± 4	347.51 ± 2
Radius of gyration (nm)	12.7 ± 0.2	12.8 ± 0.2	13.1 ± 0.3	12.9 ± 0.2	13.7 ± 0.4	12.9 ± 0.5
	ANTHRACITE (ANT)					
Volume fraction (m^3/m^3)	0.591 ± 0.1	0.591 ± 0.1	0.660 ± 0.1	0.742 ± 0.1	0.964 ± 0.1	0.884 ± 0.1
Specific surface area (m^2/cm^3)	333.62 ± 3	332.74 ± 4	268.51 ± 3	243.11 ± 3	84.95 ± 5	125.32 ± 3
Radius of gyration (nm)	12.3 ± 0.3	12.7 ± 0.3	11.8 ± 0.3	11.4 ± 0.5	12.1 ± 0.2	13.1 ± 0.4

temperature for all coal chars regardless of the rank. A transformational change of 0.11 Å was observed for LIG; 0.12 Å for SUB; 0.10 for BIT-LV; 0.05 Å for BIT-HV; 0.05 Å for SA and 0.05Å for ANT. The lateral adjustment in the value of the interlayer spacing for all the coal chars can be due to re-alignment of the basic structural units of the coal matrix which leads to the chars becoming more ordered and condensed [17] [19] [26] [33] [34]. Lu *et al.* has reported that the interlayer spacing is strongly affected by heat treatment temperature of 900˚C and above, and this result into a decrease in the interlayer spacing which invariably amounts to a more condensed char structure [34]. The condensed structure of the char is attributed to the removal of aliphatic side chains from the coal matrix and the reduction of hydrogen content which makes room for hydrogen radicals to re-combine forming higher aromatic molecules at higher temperatures [26].

The aromaticity was determined to be in range of 0.66 to 0.76 for LIG; 0.67 to 0.80 for SUB; 0.91 to 0.99 for BIT-LV; 0.93 to 0.99 for BIT-HV; 0.96 to 0.99 for SA and 0.96

Table 4. Pore size distribution, porosity and DR surface area for the different char suites.

LIG CHAR	450	500	550	600	650	700
Macro (%)	29 ± 0.1	36 ± 0.3	24 ± 0.2	32 ± 0.1	27 ± 0.3	29 ± 0.2
Meso (%)	68 ± 0.2	61 ± 0.3	70 ± 0.2	61 ± 0.1	65 ± 0.3	58 ± 0.1
Micro (%)	3 ± 0.3	3 ± 0.1	6 ± 0.3	7 ± 0.2	8 ± 0.3	13 ± 0.4
Porosity (%)	13 ± 0.2	16 ± 0.1	25 ± 0.2	30 ± 0.3	22 ± 0.1	15 ± 0.3
DR Surface area (m^2/g)	285 ± 3	323 ± 2	381 ± 4	414 ± 3	451 ± 2	475 ± 1
SUB CHAR						
Macro (%)	39 ± 0.3	43 ± 0.1	40 ± 0.2	41 ± 0.3	41 ± 0.1	42 ± 0.3
Meso (%)	59 ± 0.1	54 ± 0.1	56 ± 0.3	55 ± 0.1	51 ± 0.2	47 ± 0.3
Micro (%)	2 ± 0.2	3 ± 0.3	4 ± 0.2	4 ± 0.3	8 ± 0.4	11 ± 0.1
Porosity (%)	11 ± 0.3	13 ± 0.1	14 ± 0.2	19 ± 0.3	20 ± 0.2	19 ± 0.3
DR Surface area (m^2/g)	246 ± 2	291 ± 3	342 ± 2	387 ± 3	405 ± 3	413 ± 2
BIT-LV CHAR						
Macro (%)	31 ± 0.1	34 ± 0.3	35 ± 0.2	27 ± 0.3	30 ± 0.2	30 ± 0.3
Meso (%)	50 ± 0.2	52 ± 0.3	52 ± 0.2	53 ± 0.3	55 ± 0.2	58 ± 0.1
Micro (%)	19 ± 0.4	14 ± 0.1	13 ± 0.2	20 ± 0.3	15 ± 0.1	12 ± 0.3
Porosity (%)	11 ± 0.3	14 ± 0.2	20 ± 0.3	21 ± 0.2	20 ± 0.3	19 ± 0.1
DR Surface area (m^2/g)	243 ± 3	253 ± 2	333 ± 4	338 ± 3	374 ± 2	402 ± 1
BIT-HV CHAR						
Macro (%)	29 ± 0.1	34 ± 0.3	38 ± 0.2	30 ± 0.2	34 ± 0.1	29 ± 0.3
Meso (%)	52 ± 0.3	51 ± 0.1	52 ± 0.4	61 ± 0.2	60 ± 01	59 ± 0.3
Micro (%)	19 ± 0.2	15 ± 0.3	10 ± 0.2	9 ± 0.3	8 ± 0.1	12 ± 0.3
Porosity (%)	12 ± 0.3	15 ± 0.1	17 ± 0.1	19 ± 0.4	23 ± 0.2	21 ± 0.3
DR Surface area (m^2/g)	206 ± 2	253 ± 4	294 ± 2	331 ± 3	347 ± 2	361 ± 3
SA CHAR						
Macro (%)	34 ± 0.2	29 ± 0.1	31 ± 0.2	31 ± 0.3	31 ± 0.4	19 ± 0.3
Meso (%)	51 ± 0.3	57 ± 0.3	56 ± 0.3	64 ± 0.3	59 ± 0.3	65 ± 0.3
Micro (%)	15 ± 0.1	14 ± 0.4	13 ± 0.1	5 ± 0.2	10 ± 0.2	16 ± 0.3
Porosity (%)	14 ± 0.1	15 ± 0.1	17 ± 0.3	18 ± 0.2	23 ± 0.3	22 ± 0.1
DR Surface area (m^2/g)	221 ± 3	234 ± 2	274 ± 2	300 ± 3	313 ± 2	368 ± 4
ANT CHAR						
Macro (%)	25 ± 0.2	23 ± 0.3	19 ± 0.2	13 ± 0.3	14 ± 0.1	23 ± 0.3
Meso (%)	60 ± 0.4	62 ± 0.2	68 ± 0.1	74 ± 0.2	63 ± 0.3	64 ± 0.3
Micro (%)	15 ± 0.2	15 ± 0.3	13 ± 0.1	13 ± 0.1	23 ± 0.3	13 ± 0.4
Porosity (%)	11 ± 0.3	14 ± 0.1	15 ± 0.3	16 ± 0.2	21 ± 0.2	17 ± 0.3
DR Surface area (m^2/g)	210 ± 2	218 ± 4	221 ± 2	241 ± 3	262 ± 2	263 ± 3

to 0.99 for ANT. The transformational change in aromaticity was determined to be 0.1 for LIG; 0.13 for SUB; 0.08 for BIT-LV; 0.06 for BIT-HV; 0.03 for the anthracitic group (SA and ANT) respectively. The aromaticity was found to increase with increasing

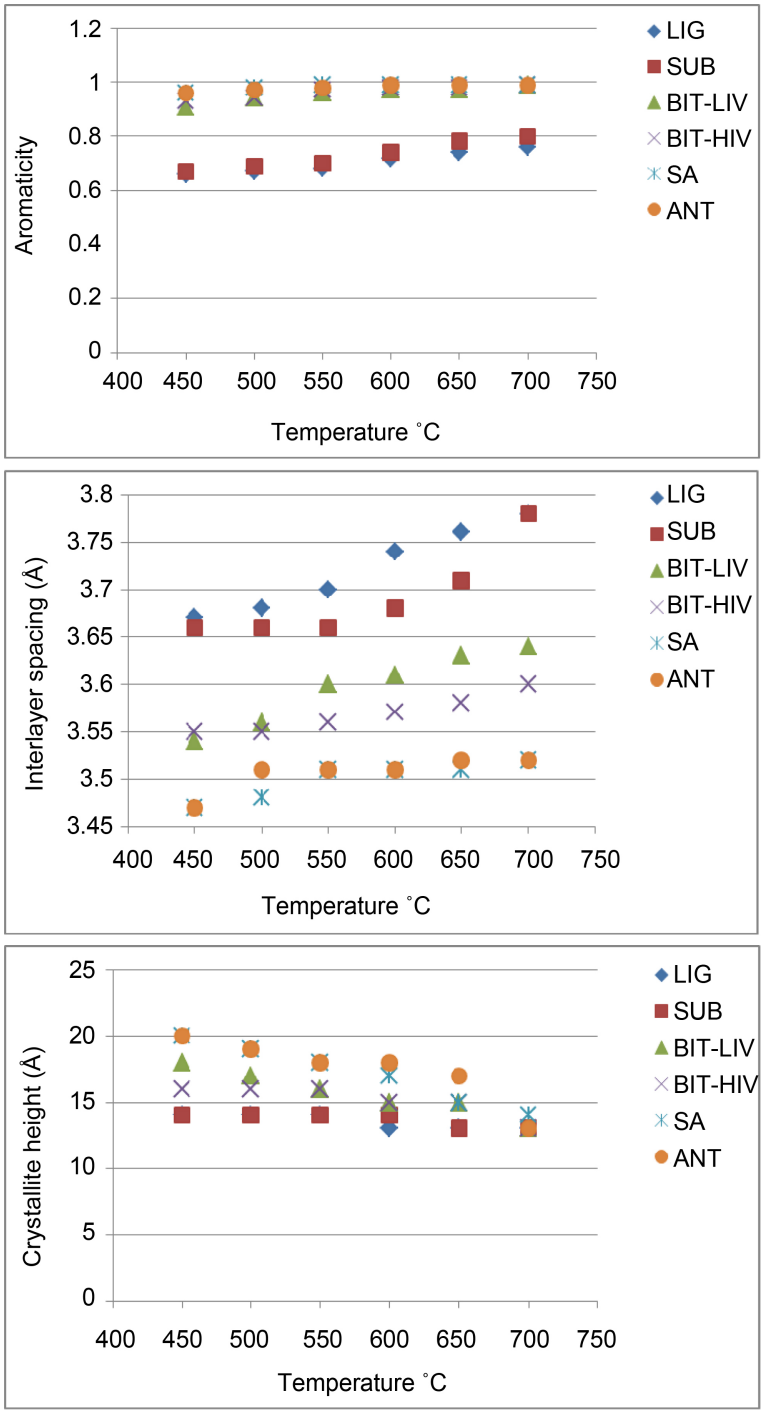

Figure 1. Variation of char's chemical properties with temperature.

pyrolysis temperature for all coal char as a result of the breaking off of the side aliphatic chain carbons [33]. The gradual increase in aromaticity with increasing temperature was more pronounced for the low rank coals due to the fact that the aliphatic side chains are not strongly bonded to the coal matrix. Similar trend was also observed for the medium rank coals as the bond to the coal matrix is not as firm as with the high

rank coals.

As the data in Table 3 and Figure 2 show, the specific surface area did not demonstrate any given trend with coal rank and increasing pyrolysis temperature, rather it was a dramatic display of values from the lowest to the highest pyrolysis temperature. However, it can be observed that the semi-anthracite coal (SA) has the highest value of 348 m^2/cm^3 at the final pyrolysis temperature of 700˚C. This implies that this coal sample is the most reactive of the coals examined, since it has the largest volume of active sites for reaction to take place at high temperatures [31] [38]. The trend of increasing reactivity was followed by the two medium rank coals, having specific surface area value of 242 m^2/cm^3 and 248 m^2/cm^3 for BIT-LV and BIT-HV. The surface area was determined to be 260 m^2/cm^3 for LIG; 239 m^2/cm^3 for SUB and 125 m^2/cm^3 for ANT. From a quantitative point of view and considering the highest pyrolysis temperature of 700˚C, the data suggests that the reactivity order of the examined coals may be represented as:

$$SA > LIG > BIT\text{-}HV > BIT\text{-}LV > SUB > ANT$$

In contrast to this observation at 700˚C, at lower heating temperature of 450˚C, and as expected from literatures due to the fact that coals were acid washed, the two medium rank coals were more reactive than the low and high rank coals. This could be

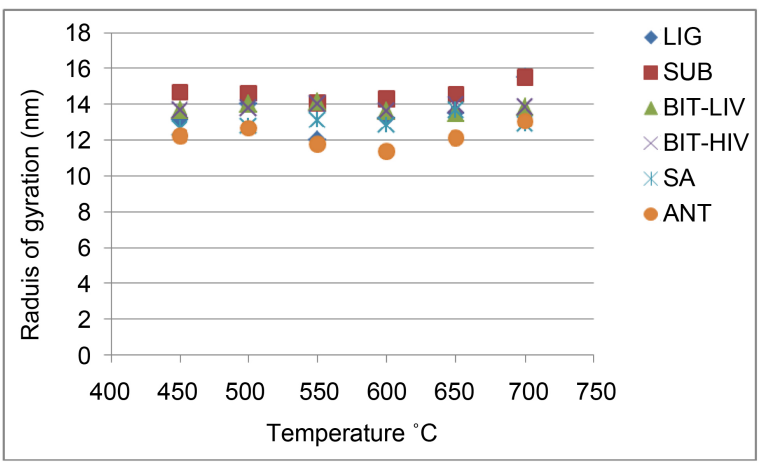

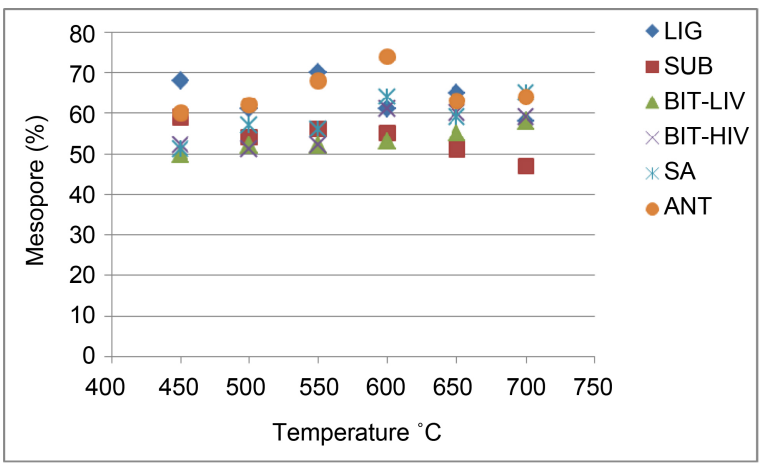

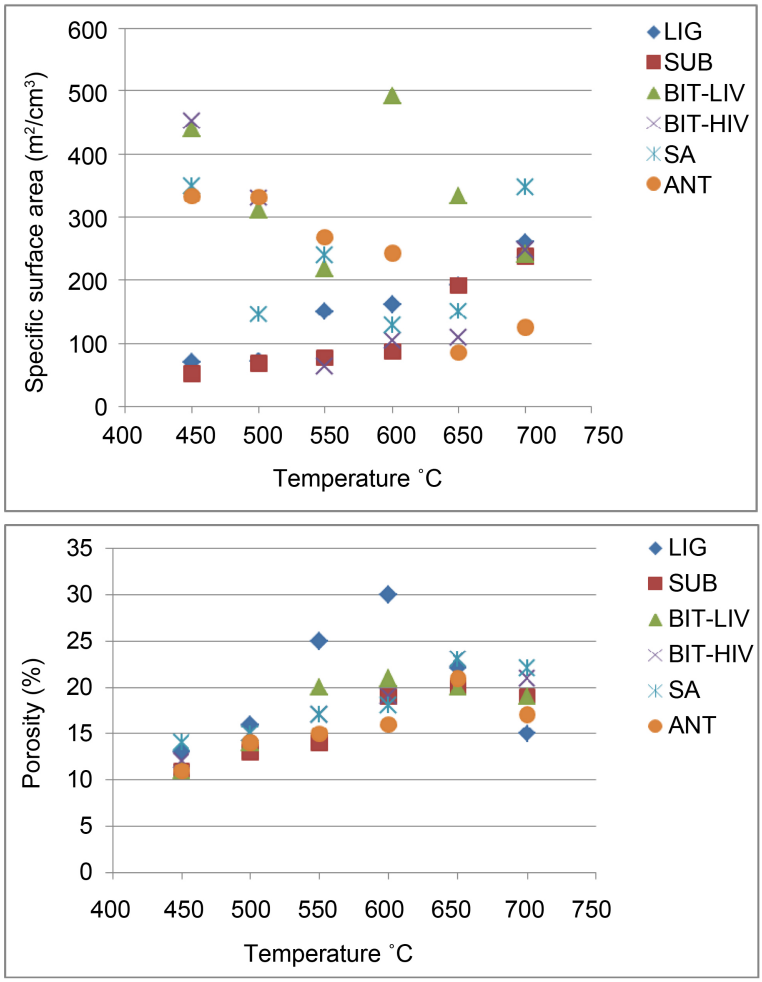

Figure 2. Variation of char's physical properties with temperature.

attributed to the washing off of the alkaline and alkaline earth metals in the low rank coals that aids coal reaction [38] and the inactivity of the active minerals present in the high rank coals [39]. Though considerable variation was seen in the values of the specific surface area between coals from low to high pyrolysis temperature, the results fit well with published rank trends [40], and when the conventional properties (proximate and ultimate analyses data) are put into consideration [38].

As can also be seen in **Table 3** and **Figure 2**, the radius of gyration (a parameter proportional to the surface area) increased gradually with increasing pyrolysis temperature and was more pronounced for the low rank coals. Though the pattern of increase did not exhibit any defined trend but of interest, it was observed that the two low rank coals converged to the same value of 15.50 nm (155 Å) at the final pyrolysis temperature of 700˚C. The two medium rank coals converged to the same value of 13.86 nm (139 Å) while the two high rank coals converged to the same value of 13.00 nm (130 Å) at the highest pyrolysis temperature of 700˚C. It is evident that the convergence to the same value by coals of same rank is a clear display of the mechanism of devolatilization and a demonstration of a decreasing anisotrophy tendency of the coals with increasing

pyrolysis temperature as expected due to the complex character in coal and coal chars [23] [32] [38]. Coals of same rank seem to exhibit same devolatilization mechanisms that lead to more aromatic structure of the coal matrix where the size and the thickness of the carbon sheets increase with the heating temperature [41] [42]. Thus, as the rank of the coal increases, the radius of gyration decreases.

Table 4 and Figure 3 give the pore size distribution and porosity of the different coal

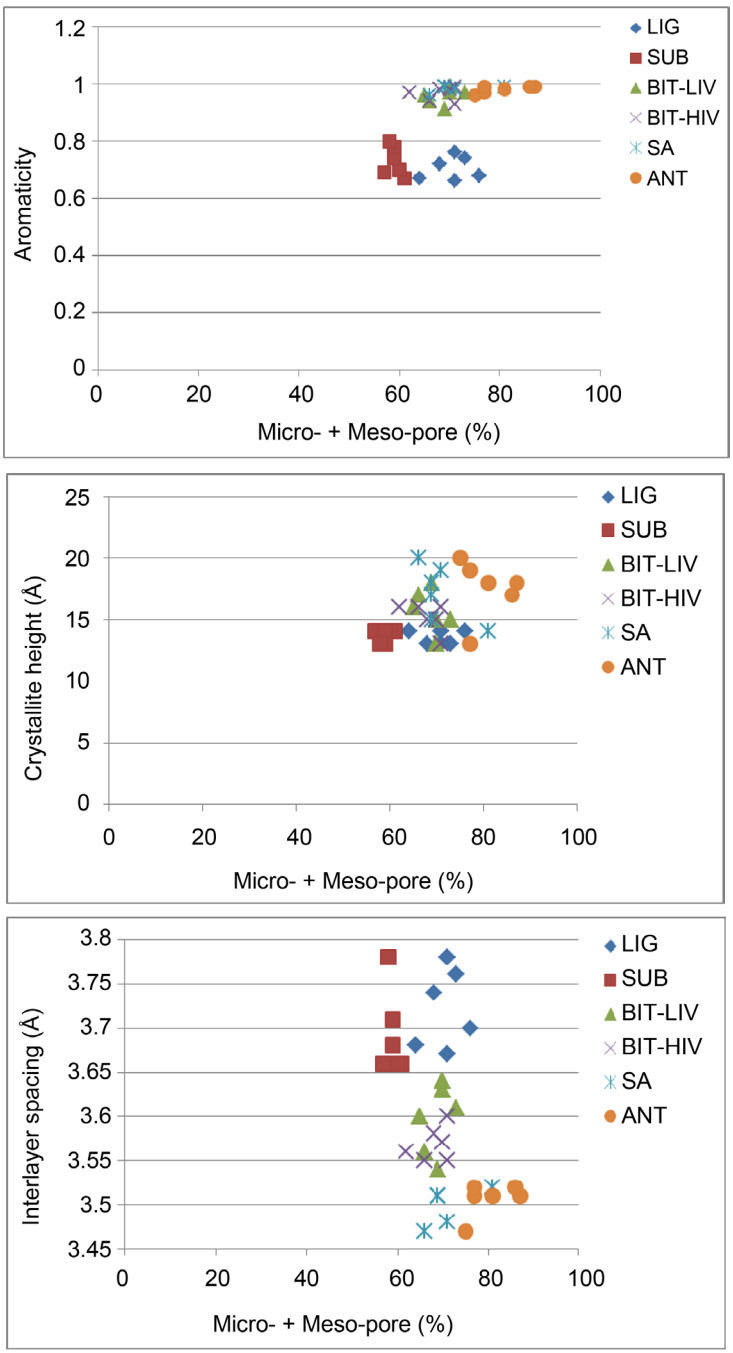

Figure 3. Variation of crystallite features with micro- + meso-pore concentration.

char suites. As can be seen, there seems to be no contribution from the macropores and little contribution from the micropores, hence, the discussion in this paper will be focused on the mesopores (the major contributor to the reaction). Similar reference to the importance of the mesopore group during coal conversion processes has been reported in the work of Jagtoyen [43]. **Table 3** also reveals that there is no common pattern of the contribution of the mesopores to the pyrolysis process among the coals of different rank. The mesopores was determined to be 68% at the lowest pyrolysis temperature for LIG and 58% at the highest pyrolysis temperature, implying the 10% of the pores were consumed in the process. The mesopores was determined to be 59% at 450˚C and 47% at 700˚C for SUB, with a transformational change of 12% pore consumption. The transformational change was determined to be 8% pore growth for BIT-LV; 7% pore growth for BIT-HV; 14% pore growth for SA and 4% pore growth for ANT. Pores in coals have a broad size distribution and form a constricted, interconnected network which defines the channels and pathways for fluids to move into and interact with the macromolecular structure of coals. Hence, porosity along with the surface area is considered as key parameters in the technical performance evaluation of coal during its utilization processes such as in fixed bed gasification. As can be seen in **Table 4**, the porosity in the lower ranked lignite and sub-bituminous coals is primarily in the form of macropores, which is considered as primary porosity. For the intermediate ranked bituminous coals, loss of primary porosity sets in and the evolution of secondary porosity (micro- and meso-porosity) starts such that 80% of the accessible porosity is contributed by micro- and meso-pores [43]. While in the higher ranked semi-anthracite and anthracite coals, micro-porosity predominates. Therefore, it could be inferred that, as the rank of the coal increases, the importance of macro-porosity decreases and micro-porosity becomes increasingly significant. **Figure 3** reveals that coal porosity and pore size distribution varies with the degree of maturity of coals as measured by the indictors: aromaticity, interlayer spacing and crystallite height.

Again, aligning this result of pore size distribution with the analysis of specific surface area confirms the SA coal as the most reactive of the coals investigated. Previous work by Mare and co-workers has reported that porosity is predominantly composed of microporosity, which contributed the majority of the available specific surface area to the pyrolysis process [30] [44], but this is contrary to what was obtained in this study as revealed in **Table 4**, inferring that majority of the contribution to specific surface area comes from the mesopores. As reported in Gibaud *et al.* [42] and experienced in this study, the macropore surface area does not change significantly as a function of the heat-treatment temperature [45], while the micropore surface area does not change significantly upon further heating, above 700˚C. The lower mesopore-micropore range (daimeter of 5 to 175 Å) [31] for some carbonaceous materials such as coal have been associated with the inter-layer spacing in clay minerals [43], based on this fact, a plot of combined mesopore-micropore was constructed against the crystallite properties of the coals examined in this investigation to established some links as can be seen in **Figure 3**. No correlation was established, and this can be attributed to the complicated nature

of coal and coal char [28].

As the data in Table 4 show, the porosity increases with increasing pyrolysis temperature to a maximum value. Apart from the LIG and BIT-LV coals that had a fall after 600˚C, the other coals experienced the decrease after 650˚C. The maximum porosity was determined to be 30% for LIG, 20% for SUB; 21% for BIT-LV; 23% for BIT-HV; 23% for SA and 21% for ANT. If porosity would have been used for coal reactivity assessment as obtained in this work, LIG would have been assumed to be the more reactive, which is not the case in this investigation. This reinforces the notion that a range of rank-related factors (of which porosity is an important one) contributes to the high relative reactivity of low-rank coals such as lignite [45].

Char micropore surface area was measured using adsorption of CO_2 at 273 K and data analysis using the Dubinin-Radushkevich (DR) method is presented in Table 4 and as can be seen in Figure 4; a plot of the DR micropore against the char crystallite features reveals an almost linear relationship, consistent with what one might expect based on the relative ranks of the parent coals (Table 1). The low ranked lignite and sub-bituminous coals exhibited the highest volumes of micropores among the coal samples used in this study. The transformational change in the volume of the micropores was also more pronounced for the low rank coals than the higher rank coals. Thus, the micropores available for coal reaction during utilization processes increases with coal maturity as reflected in Figure 4. However, the limitation of CO_2 adsorption technique in measuring coal and coal char surface areas, is that it only probes the micropore size range and thus cannot be used independently to describe the overall porosity or pore size distribution of coal and coal char. Results obtained from CO_2, N_2 and Mercury porosimetry are usually combined to obtain a complete description of the pore structure, surface area and porosity of coal [31]. SAXS has the advantage of probing a wider range of pore sizes in a single experiment than the gas adsorption (CO_2 and N_2) or Mercury porosimetry methods.

As can be seen in Figure 5, the relationship between the chemical and physical properties of coal during pyrolysis was established only for aromaticity and the physical properties that gave definite good correlation. Evidence from other works reported this demonstration of the transition from amorphous aliphatic fraction to a more condensed aromatic fraction to be attributed to the loss of components having higher proportions of oxygen, hydrogen and disorganized carbon as the transition progress from low to high temperatures [4]-[6] [8] [11] [19]-[21] [25] [29]. Moreover, the structural significance of this relationship cannot be over-emphasized in the interpretation of the reactivity of coal char, even when the fundamental physical parameters does not change in a straightforward way as graphitization proceeds (increase in aromaticity). As depicted in Figure 5, the aromaticity: which is one of the parameters used in measuring the chemical stability of coal transformation stands as a good indicator of coal maturity because of the realignment of the carbon molecules gave definite relationship with the coal physical properties of specific surface area, mesopore and porosity, which was more pronounced for the low rank coals [38] [39].

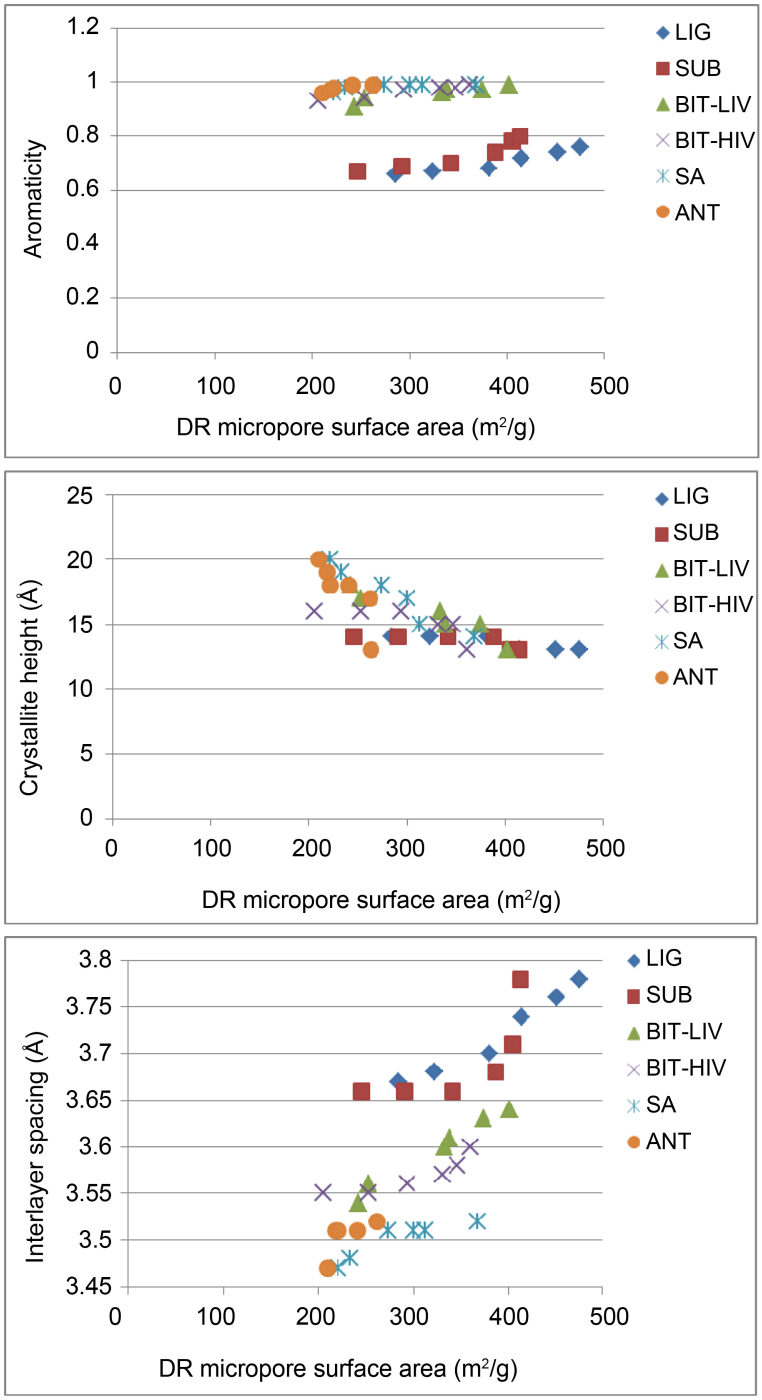

Figure 4. Variation of crystallite features with DR surface area.

4. Concluding Remarks

Investigations of six different coals of different rank were performed in order to evaluate the relationship between char morphology and its chemical properties with non-invasive techniques of SAXS and XRD respectively. Although both analytical techniques offer interesting perspective for the thermal analysis of coal (internal and external

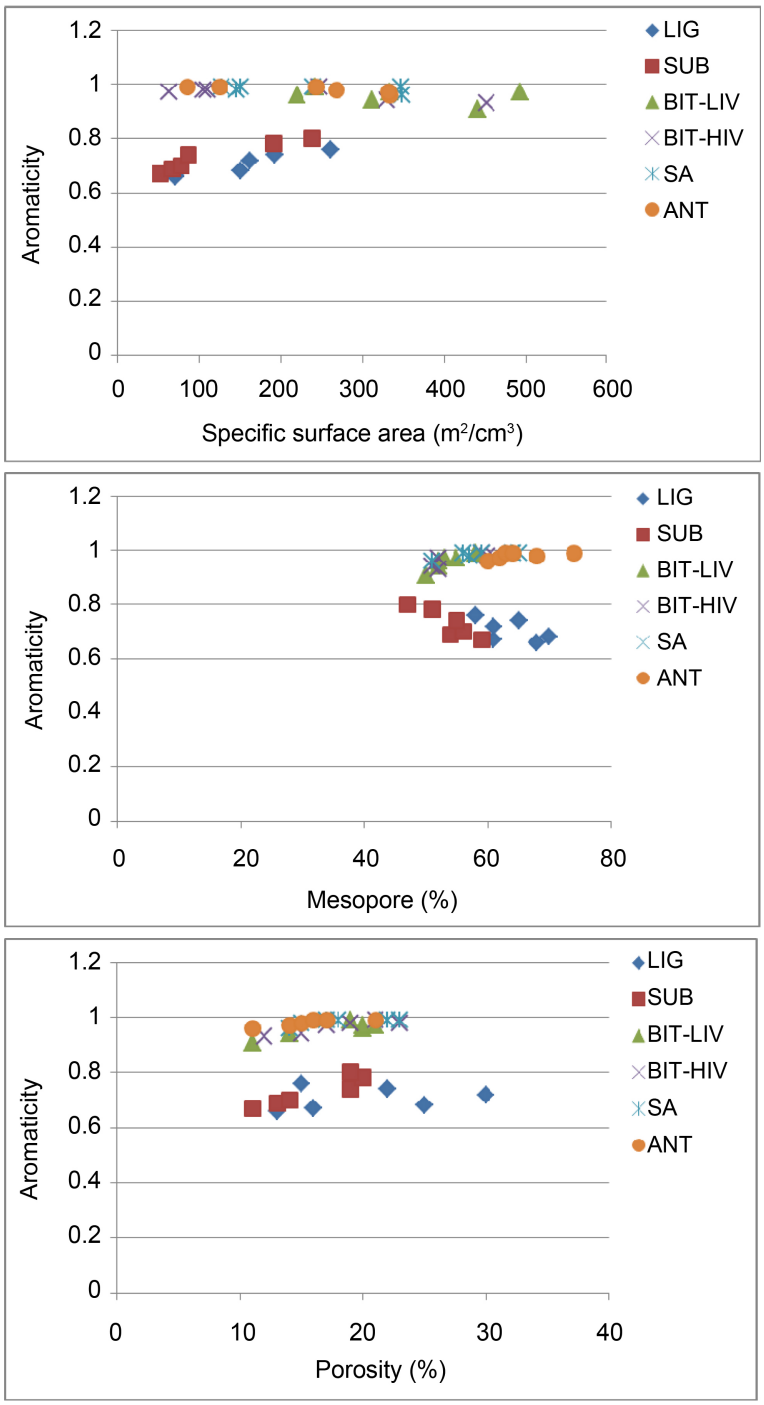

Figure 5. Plot of aromaticity against char's physical properties.

features), it is realized that fractal dimension of the surface of a porous solid does not depend, theoretically on the size of the pores or the amount of surface but rather is an intrinsic characteristic of the surface itself but rather depends on other coal properties such as petrographic composition. Physically, the specific surface area obtained using SAXS role in determining the reactivity of a coal cannot be undermined as it reveals the

accessible surface available for reaction. The crucial nature of SAXS analysis reveals the possibility of evaluating char reactivity based on its morphology from a single analytical technique without relying on the combination of other analytical techniques such as adsorption method (CO_2 and N_2) and mercury porosimetry. As far as the author could assess, this is a novel finding, the use of the SAXS analytical technique to assess the reactivity of coal char. Demineralization produced a material whose pore size distribution as determined by SAXS and aromaticity as determined by XRD is that of the organic component of the coal. Of the chemical properties obtained from the XRD, only the aromaticity gave a definite relationship with the physical properties obtained by SAXS. This is generally attributed to the increase in aromaticity as a result of loss of aliphatic, carboxyl, and carbonyl groups from the carbonaceous material and the fact that SAXS probes a wider range of pores, including pores that are closed to, or restricted in access by other techniques such as gas adsorption or mercury intrusion.

Acknowledgements

The work presented in this paper is based on the research supported by the South African Research Chairs Initiative of the Department of Science and Technology and National Research Foundation of South Africa (Coal Research Chair Grant No. 86880). Any opinion, finding or conclusion or recommendation expressed in this material is that of the author and the NRF does not accept any liability in this regard.

References

[1] Hefta, R.S., Schobert, H.H. and Kube, W.R. (1986) Calorimetric Pyrolysis of a North Dakota Lignite. *Fuel*, **65**, 1196-1202. http://dx.doi.org/10.1016/0016-2361(86)90229-2

[2] Morgan, P.A., Robertson, S.D. and Unswort, J.F. (1987) Combustion Studies by Thermogravimetric Analysis. *Fuel*, **66**, 210-215. http://dx.doi.org/10.1016/0016-2361(87)90243-2

[3] Liu, G., Benyon, P., Benfell, K.E., Bryant, G.W., Tate, A.G., Boyd, R.K., Harris, D.J. and Wall, T.F. (2000) The Porous Structure of Bituminous Coal Chars and Its Influence on Combustion and Gasification under Chemically Controlled Conditions. *Fuel*, **79**, 617-626. http://dx.doi.org/10.1016/S0016-2361(99)00185-4

[4] Bai, Y., Wang, Y., Zhu, S., Li, F. and Xie, K. (2014) Structural Features and Gasification Reactivity of Coal Chars Formed in Ar and CO_2 Atmospheres at Elevated Pressures. *Energy*, **74**, 464-470. http://dx.doi.org/10.1016/j.energy.2014.07.012

[5] Bar-Ziv, E. and Kantorovich, I.I. (2001) Mutual Effects of Porosity and Reactivity in Char Oxidation. *Progress in Energy and Combustion Science*, **27**, 667-697. http://dx.doi.org/10.1016/S0360-1285(01)00006-5

[6] Kulaots, I., Hsu, A. and Suuberg, E.M. (2007) The Role of Porosity in Char Combustion. *Proceedings of the Combustion Institute*, **31**, 1897-1903. http://dx.doi.org/10.1016/j.proci.2006.08.004

[7] Yokono, T., Miyazawa, K. and Sanada, Y. (1978) Aromaticity of Coal Extract by IH and 13C Pulsed n.m.r. Methods. *Fuel*, **57**, 555-558. http://dx.doi.org/10.1016/0016-2361(78)90041-8

[8] Sonibare, O.O., Haeger, T. and Foley, S.F. (2010) Structural Characterization of Nigerian Coals by X-Ray Diffraction, Raman and FTIR Spectroscopy. *Energy*, **35**, 5347-5353.

http://dx.doi.org/10.1016/j.energy.2010.07.025

[9] Li, Y., Cao, X., Zhu, D., Chappell, M.A., Miller, L.F. and Mao, J. (2012) Characterization of Coals and Their Laboratory-Prepared Black Carbon Using Advanced Solid-State ^{13}C Nuclear Magnetic Resonance Spectroscopy. *Fuel Processing Technology*, **96**, 56-64. http://dx.doi.org/10.1016/j.fuproc.2011.12.014

[10] Lu, L., Sahajwalla, V., Kong, C. and Harris, D. (2001) Quantitative X-Ray Diffraction Analysis and Its Application to Various Coals. *Carbon*, **39**, 1821-1833. http://dx.doi.org/10.1016/S0008-6223(00)00318-3

[11] Jones, J.M., Pourkashanian, M., Rena, C.D. and Williams, A. (1999) Modelling the Relationship of Coal Structure to Char Porosity. *Fuel*, **78**, 1737-1744. http://dx.doi.org/10.1016/S0016-2361(99)00122-2

[12] Li, W., Zhu, Y., Chen, S. and Zhou, Y. (2013) Research on the Structural Characteristics of Vitrinite in Different Coal Ranks. *Fuel*, **107**, 647-652. http://dx.doi.org/10.1016/j.fuel.2012.10.050

[13] Kulaots, I., Aarna, I., Callejo, M., Hurt, R.H. and Suuberg, E.M. (2002) Development of Porosity during Coal Char Combustion. *Proceedings of the Combustion Institute*, **29**, 495-501. http://dx.doi.org/10.1016/S1540-7489(02)80064-5

[14] Aarna, I. and Suuberg, E.M. (1999) Two Kinetic Regime Behavior in Carbon Dioxide Gasification of Carbons. *Carbon*, **37**, 147-163. http://dx.doi.org/10.1016/S0008-6223(98)90103-8

[15] Zhang, S., Zhu, F., Bai, C., Wen, L. and Zou, C. (2013) Thermal Behavior and Kinetics of the Pyrolysis of the Coal Used in the COREX Process. *Journal of Analytical and Applied Pyrolysis*, **104**, 660-666. http://dx.doi.org/10.1016/j.jaap.2013.04.014

[16] Zhang, C., Jiang, X., Wei, L. and Wang, H. (2007) Research on Pyrolysis Characteristics and Kinetics of Super Fine and Conventional Pulverized Coal. *Energy Conversion and Management*, **48**, 797-802. http://dx.doi.org/10.1016/j.enconman.2006.09.003

[17] Calo, J.M. and Hall, P.J. (2004) The Application of Small Angle Scattering Techniques to Porosity Characterization in Carbons. *Carbon*, **42**, 1299-1304. http://dx.doi.org/10.1016/j.carbon.2004.01.030

[18] Liu, Q., Hu, H., Zhou, Q., Zhu, S. and Chen, G. (2004) Effect of Inorganic Matter on Reactivity and Kinetics of Coal Pyrolysis. *Fuel*, **83**, 713-718. http://dx.doi.org/10.1016/j.fuel.2003.08.017

[19] Alonso, M.J.G., Borrego, A.G., Alvarez, D., Kalkreuth, W. and Menendez, R. (2001) Physicochemical Transformations of Coal Particles during Pyrolysis and Combustion. *Fuel*, **80**, 1857-1870. http://dx.doi.org/10.1016/S0016-2361(01)00071-0

[20] Wiktorsson, L.-P. and Wanzl, W. (2000) Kinetic Parameters of Coal Pyrolysis at Low and High Heating Rates: A Comparison of Data from Different Laboratory Equipment. *Fuel*, **79**, 701-716. http://dx.doi.org/10.1016/S0016-2361(99)00138-6

[21] Alonso, M.J.G., Borrego, A.G., Alvarez, D., Parra, J.B. and Menendez, R. (2001) Influence of Pyrolysis Temperature on Char Optical Texture and Reactivity. *Journal of Analytical and Applied Pyrolysis*, **58-59**, 887-909. http://dx.doi.org/10.1016/S0165-2370(00)00186-8

[22] Kelepobile, L., Sun, R., Wang, H., Zhang, X. and Wu, S. (2013) Pore Development and Combustion Behavior of Gasified Semi-Char in a Drop Tube Furnace. *Fuel Processing Technology*, **111**, 42-54. http://dx.doi.org/10.1016/j.fuproc.2013.01.017

[23] Nguyen, T.X. and Bhatia, S.K. (2012) Characterization of Accessible and Inaccessible Pores in Microporous Carbons by a Combination of Adsorption and Small Angle Neutron Scattering. *Carbon*, **50**, 3045-3054. http://dx.doi.org/10.1016/j.carbon.2012.02.091

[24] Geng, W., Nakajima, T., Takanashi, H. and Ohki, A. (2009) Analysis of Carboxyl Group in Coal and Coal Aromaticity by Fourier Transform Infrared (FT-IR) Spectroscopy. *Fuel*, **88**, 139-144. http://dx.doi.org/10.1016/j.fuel.2008.07.027

[25] Borrego, A.G., Osorio, E., Casal, M.D. and Vilela, A.C.F. (2008) Coal Char Combustion under a CO_2-Rich Atmosphere: Implications for Pulverized Coal Injection in a Blast Furnace. *Fuel Processing Technology*, **89**, 1017-1024. http://dx.doi.org/10.1016/j.fuproc.2008.03.012

[26] Melnichenko, Y.B., Radlinski, A.P., Mastarlerz, M., Cheng, G. and Rupp, J. (2009) Characterization of the CO_2 Fluid Adsorption in Coal as a Function of Pressure Using Neutron Scattering Techniques (SANS and USANS). *International Journal of Coal Geology*, **77**, 69-79. http://dx.doi.org/10.1016/j.coal.2008.09.017

[27] Yao, Y., Liu, D., Tang, D., Tang, S. and Huang, W. (2008) Fractal Characterization of Adsorption-Pores of Coals from North China: An Investigation on CH_4 Adsorption Capacity of Coals. *International Journal of Coal Geology*, **73**, 27-42. http://dx.doi.org/10.1016/j.coal.2007.07.003

[28] Du, X. and Wu, E. (2007) Porosity of Microporous Zeolites A, X and ZSM-5 Studied by Small Angle X-Ray Scattering and Nitrogen Adsorption. *Journal of Physics and Chemistry of Solids*, **68**, 1692-1699. http://dx.doi.org/10.1016/j.jpcs.2007.04.013

[29] Chan, M.-L., Jones, J.M., Pourkashanian, M. and Willaims, A. (1999) The Oxidative Reactivity of Coal Chars in Relation to Their Structure. *Fuel*, **78**, 1539-1552. http://dx.doi.org/10.1016/S0016-2361(99)00074-5

[30] Stoeckli, F., Guillot, A., Slasli, A.M. and Hugi-Cleary, D. (2002) The Comparison of Experimental and Calculated Pore Size Distributions of Activated Carbons. *Carbon*, **40**, 383-388. http://dx.doi.org/10.1016/S0008-6223(01)00115-4

[31] Radlinski, A.P., Busbridge, T.L., Gray, E.M.A., Blach, T.P. and Cookson, D.J. (2009) Small Angle X-Ray Scattering Mapping and Kinetics Study of Sub-Critical CO_2 Sorption by Two Australian Coals. *International Journal of Coal Geology*, **77**, 80-89. http://dx.doi.org/10.1016/j.coal.2008.09.015

[32] Sastry, P.U., Sen, D., Mazumder, S. and Chandrasekaran, K.S. (2000) Structural Variations in Lignite Coal: A Small Angle X-Ray Scattering Investigation. *Solid State Communications*, **114**, 329-333. http://dx.doi.org/10.1016/S0038-1098(00)00060-0

[33] Lu, L., Sahajwalla, V., Kong, C. and Harris, D. (2001) Quantitative X-Ray Diffraction Analysis and Its Application to Various Coals. *Carbon*, **39**, 1821-1833. http://dx.doi.org/10.1016/S0008-6223(00)00318-3

[34] Lu, L., Sahajwalla, V., Kong, C. and Harris, D. (2000) Characteristics of Chars Prepared from Various Pulverized Coals at Different Temperatures Using Drop tube Furnace. *Energy & Fuels*, **14**, 869-876. http://dx.doi.org/10.1021/ef990236s

[35] Hattingh, B.B., Everson, R.C., Neomagus, H.W.J.P. and Bunt, J.R. (2011) Assessing the Catalytic Effect of Coal Ash Constituents on the CO_2 Gasification Rate of High Ash, South African Coal. *Fuel Processing Technology*, **92**, 2048-2054. http://dx.doi.org/10.1016/j.fuproc.2011.06.003

[36] Dangyu, S., Cunbei, Y., Xiaokui, Z., Xianbo, S. and Xiaodong, Z. (2011) Structure of the Organic Crystallite Unit in Coal as Determined by X-Ray Diffraction. *Mineral Science and Technology*, **21**, 667-671.

[37] Mares, T.E., Radlinski, A.P., Moore, T.A., Cookson, D., Thiyagarajan, P., Ilavsky, J. and Klepp, J. (2009) Assessing the Potential for CO_2 Adsorption in a Subbituminous Coal, Huntly Coalfield, New Zealand, Using Small Angle Scattering Techniques. *International Journal of Coal Geology*, **77**, 54-68. http://dx.doi.org/10.1016/j.coal.2008.07.007

[38] Odeh, A. (2015) Comparative Study of the Aromaticity of the Coal Structure during the Char Formation Process under both Conventional and Advanced Analytical Techniques. *Energy & Fuels*, **29**, 2676-2684. http://dx.doi.org/10.1021/ef502672d

[39] Odeh, A. (2015) Exploring the Potential of Petrographics in Understanding Coal Pyrolysis. *Energy*, **87**, 555-565. http://dx.doi.org/10.1016/j.energy.2015.05.019

[40] Odeh, A. (2015) Qualitative and Qualitative ATR-FTIR Analysis and Its Application to Coal Char of Different Ranks. *Journal of Fuel Chemistry and Technology*, **43**, 129-137. http://dx.doi.org/10.1016/S1872-5813(15)30001-3

[41] Melnichenko, Y.B., He, L., Sakurovs, R., Kholodenko, A.L., Blach, T., Mastarlerz, M., Radlinski, A.P., Cheng, G. and Mildner, D.F.R. (2012) Accessibility of Pores in Coal to Methane and Carbon Dioxide. *Fuel*, **91**, 200-208. http://dx.doi.org/10.1016/j.fuel.2011.06.026

[42] Gibaud, A., Xue, J.S. and Dahn, J.R. (1996) A Small Angle X-Ray Scattering Study of Carbons Made from Pyrolyzed Sugar. *Carbon*, **34**, 499-503. http://dx.doi.org/10.1016/0008-6223(95)00207-3

[43] Clarkson, C.R., Solano, N., Bustin, R.M., Bustin, A.M.M., Chalmers, G.R.L., He, L., Melnichenko, Y.B., Radlinski, A.P. and Blach, T.P. (2013) Pore Structure Characterization of North American Shale Gas Reservoirs Using USANS/SANS, Gas Adsorption, and Mercury Intrusion. *Fuel*, **103**, 606-616. http://dx.doi.org/10.1016/j.fuel.2012.06.119

[44] Jagtoyen, M., Derbyshire, F., Rimmer, S. and Rathbobe, R. (1995) Relationship between Reflectance and Structure of High Surface Area Carbons. *Fuel*, **74**, 610-614. http://dx.doi.org/10.1016/0016-2361(95)98366-M

[45] Giffin, S., Littke, R., Klaver, J. and Urai, J.L. (2013) Application of BIB-SEM Technology to Characterize Macropore Morphology in Coal. *International Journal of Coal Geology*, **114**, 85-95. http://dx.doi.org/10.1016/j.coal.2013.02.009